Molecular Biotechnology (2025) 67:2660–2672
https://doi.org/10.1007/s12033-024-01227-1

ORIGINAL PAPER

Co-delivery of Liposomal Ketoconazole and Bevacizumab for Synergistical Inhibition of Angiogenesis Against Endometrial Cancer

Shanshan Wang[1] · Jinglin Miao[2] · Ping Zhu[3] · Li Xu[2]

Received: 8 September 2023 / Accepted: 20 June 2024 / Published online: 4 September 2024

Abstract
In this study, we designed a novel formulation based on liposomes for the co-delivery of cancer-derived exosome inhibitor (ketoconazole, Keto) and angiogenesis inhibitor (bevacizumab, mAb). The designed Combo-Lipo formulation was systematically characterized, exhibiting a uniform average particle size of 100 nm, as well as excellent serum and long-term physical stabilities. The cell viability assay revealed that Combo-Lipo treatment significantly reduced the viability of cancer cells compared to free drugs. Moreover, liposomes effectively inhibited angiogenic mediators and reduced tumor immune suppressive factors. The Combo-Lipo formulation demonstrated potent downregulation of angiogenic factors and synergistic effects in suppressing their production. Furthermore, liposomes inhibited tumor-associated macrophages (TAMs), leading to decreased expression of tumor-promoting factors. Together, these findings highlighted the promising characteristics of Combo-Lipo as a therapeutic formulation, including optimal particle size, serum stability, and potent anti-cancer effects, as well as inhibition of angiogenic mediators and TAMs toward treating endometrial cancer.

Keywords Endometrial cancer · Liposomes · Co-delivery · Cancer-associated fibroblasts · Tumor-associated macrophages

Introduction

Endometrial cancer has emerged as one of the harmful cancers characterized by the significant challenges of often being diagnosed at an advanced stage, resulting in significant mortality rates among women [1]. In this context, cancer-derived exosomes play significant roles in promoting and progressing various tumors [2]. Due to various bioactive molecules, such as proteins, lipids, and nucleic acids, exosomes can influence the behavior of recipient cells. Accordingly, cancer-derived exosomes act as agents for intercellular communication and promote tumor growth by enhancing cell proliferation, angiogenesis (neovascularization process to substantial tumor growth), and metastasis (spreading cancer cells to distant sites) [3, 4]. In addition, exosomes modulate the tumor microenvironment (TME) by suppressing the immune system and promoting inflammation. These attributes in the tumor can create a favorable microenvironment for tumor survival and expansion [5]. In this context, a report demonstrated that cancer-derived exosomes could be implicated in drug resistance, as they could transfer drug efflux pumps and signaling molecules to recipient cells, thereby reducing the therapeutic efficacy of anti-cancer treatments [6]. Furthermore, cancer-derived exosomes facilitate the formation of pre-metastatic niches, altering the behavior of stromal cells, such as fibroblasts, endothelial cells, and immune cells, in the target organ [7]. The exosomes released from primary tumor cells convert the macrophage in the tumor site to tumor-associated

Shanshan Wang and Jinglin Miao have equal contribution in this paper.

✉ Ping Zhu
zhuzp111@126.com

✉ Li Xu
xuli10011@163.com

[1] Department of the First Obstetrics and Gynecology, Yantai Yuhuangding Hospital, Yantai 264099, Shandong, China

[2] Department of the Third Obstetrics and Gynecology, Yantai Yuhuangding Hospital, No. 20 Yuhuangding East Road, Zhifu District, Yantai 264099, Shandong, China

[3] Department of Reproductive Medicine, Yantai Yuhuangding Hospital, No. 20 Yuhuangding East Road, Zhifu District, Yantai 264099, Shandong, China

macrophages (TAMs), an important contributor to metastasis in the development of endometrial cancer [8].

To this end, the cancer-associated fibroblasts (CAFs) play crucial roles in the TME by producing extracellular matrix (ECM) remodeling proteins and secreting growth factors and cytokines that regulate the growth and invasion of tumor cells [9, 10]. Matrix-metalloproteinases (MMPs), as inactive proenzymes, are activated through proteolytic cleavage, involving various processes essential for tumor progression, such as neovascularization, metastasis, and cell proliferation [11]. Among various MMPs, MMP-3, specifically secreted by cancer stromal fibroblasts and endothelial cells, participates in the ECM degradation and vascular remodeling [11, 12]. It should be noted that these secreted exosomes could also transform the fibroblast to CAFs [13].

Angiogenesis is one of the intrinsic processes of cancer cells closely associated with cancer metastasis [14]. In addition to various intracellularly released molecules, the cancer-derived exosomes participate in the angiogenesis process during the cancer progression, playing a significant role in cancer metastasis [15]. Angiogenesis often facilitates cancer metastasis by initially promoting the formation of new blood vessels that supply oxygen and nutrients to further form new tumor cells [16]. Noticeably, inhibiting angiogenesis plays a crucial role in cancer therapy, preventing tumor growth and metastasis [17]. Considering the critical role of exosomes, inhibiting cancer-derived exosomes is also advantageous for cancer therapy. Among various small molecules, ketoconazole (Keto), an antifungal drug, prototype imidazole, exhibited exceptional potential in inhibiting the biogenesis *of exosomes intracellularly* [18]. To this end, anti-angiogenic drugs like bevacizumab have been applied to block blood vessel formation. Considering their exceptional therapeutic potential against tumor cells, the co-delivery of exosome and angiogenesis inhibitors can curb the metastasis ability of cancer cells [19]. The eventual therapeutic effects can also block the sources of nutrients and inhibit the pro-tumor and pro-angiogenesis microenvironment.

Liposomes are lipid-based vesicles with an average size range of 50–200 nm that can encapsulate hydrophobic molecules within their lipid bilayer and hydrophilic drugs in the aqueous core [20]. Specifically, the small hydrophobic molecules can be efficiently incorporated into liposomes, in which the lipid-based structure can provide a hydrophobic environment for their stability and delivery [21]. In addition to small hydrophobic molecules, liposomes can be loaded with antibodies on their surface [22]. Motivated by these considerations, the liposomes were designed to co-deliver the exosome inhibitor (Keto) and anti-angiogenesis antibody (bevacizumab) to treat endometrial cancer. The designed Combo-Lipo formulation was systematically characterized, showcasing the morphological and stability attributes. Furthermore, the performance of the designed Combo-Lipo formulation was determined and compared their efficacy, in terms of angiogenesis inhibition and tumor immune suppressive factors, with the corresponding pure drugs.

Experimental Section

Materials

DOPC (1,2-dioleoyl-sn-glycero-3-phosphocholine), CHOL (cholesterol), and DSPE-PEG (1,2-distearoyl-sn-glycero-3-phosphoethanolamine-*N*-[methoxy(polyethylene glycol) were purchased from Avanti lipids (Alabaster, USA). All the cell lines and fetal bovine serum (FBS, 30-2020) were acquired from the American Type Culture Collection (ATCC, Manassas, USA). The Transwell system was purchased from the Corning Life Sciences (Corning, USA).

Cell Culture

Human uterine epithelial cells (RL95-2 cell line, CRL-1671) were cultured in the Dulbecco's Modified Eagle's Medium (DMEM) and F-12 Medium supplemented with 10% exosome-free FBS. HEC-1A cell line (HTB-112) was cultured in McCoy's 5A Medium (30-2007) supplemented with 10% exosome-free FBS. HEC-1B cell line (HTB-113) was cultured in the Eagle's Minimum Essential Medium (EMEM) supplemented with 10% exosome-free FBS. Human Primary Dermal Fibroblasts, referred to as non-cancerous/normal cell line (PCS-201-012™), were cultured in the Fibroblast Basal Medium (PCS-999-001) supplemented with fibroblast growth kit components (PCS-201-040) and 2% exosome-free FBS. Human cytotoxic CD8 T-cells (PCS-800-017) were cultured according to the manufacturer's instructions. Human Primary Peripheral Blood Mononuclear Cells (PBMCs) (PCS-800-011™) were thawed in the (Hank's Balanced Salt Solution without Ca^{2+} or Mg^{2+} (ATCC 30-2213) supplemented with the 10% exosome-free medium. Notably, PBMCs have a limited lifespan in culture and should be thawed shortly just before experiments. Thawing PBMCs well in advance might lead to reduced viability and functionality.

Preparation of Exosome-Free Serum

Several approaches, such as ultracentrifugation, can be employed to remove or deplete exosomes from the serum. In this study, we applied the ultracentrifugation approach to remove exosomes. Briefly, the serum was collected and centrifuged at a high speed (typically 100,000×*g* or higher) for a prolonged period to pellet the exosomes. Further, the supernatant was carefully collected and subjected to sterile filtration using a 0.22 μm filter membrane, ensuring the

serum was free from contaminants. Finally, the aliquots of exosome-free serum were separated and stored at − 80 °C to maintain their stability and prevent degradation until further use.

Preparation and Characterization of Liposomes

The drug was loaded into the liposomes via thin film dispersion method, which is commonly used for hydrophobic drug [29]. Initially, the lipids at a below weight ratio were dissolved in dichloromethane (DCM). Further, the organic solvent was evaporated under a vacuum at 60 °C, ensuring complete removal of the organic solvent. Eventually, the lipid film was hydrated by adding 2 mL of distilled water, and the hydration process was performed at a temperature of 60 °C for 30 min. The formulation was optimized according to the ratio in Table 1 and F2 was chosen for further liposome preparation in this study. Blank liposome (DOPC:CHOL:DSPE-PEG:Keto = 6:2:1) was used as the vehicle control. The uniform-sized liposomes were prepared by subjecting the mixture to the extrusion process. The hydrodynamic size, polydispersity index (PDI), and zeta potential of the prepared liposomes were assessed using dynamic light scattering (DLS) with the Zetasizer Nano ZS 90 instrument (Malvern Co., Ltd., U.K.). The long-term stability of liposomes in serum-free condition was evaluated at 4 °C. The stability of liposomes in 5% goat serum at 37 °C was also evaluated. The drug release study was conducted at the 0.1% tween-PBS.

Cell Viability Assay

The cell viability was assessed using the 3-(4,5-dimethylthiazol-2-yl)-2,5-diphenyltetrazolium bromide (MTT) assay. HEC-1B, HEC-1A, and RL95-2 cancer cells at the logarithmic phase were seeded in the 96-well plates at a density of 5000 per well and incubated overnight for proper attachment to the surface. Then, the wells were added with formulations, including free Keto, Keto-Lipo, bevacizumab (mAb), and Combo-Lipo (liposomes co-loaded with Keto and bevacizumab). All the treatment groups of cells were treated with the same dose of Keto at 2 μM and bevacizumab at 4 μg mL^{-1} and incubated for 48 h. A stock solution of MTT (5 mg mL^{-1}) in sterile PBS was prepared. Further, the culture medium was removed from the cells, and the MTT solution (working concentration of 0.5 mg mL^{-1}) was added to each well. The cells were then incubated with the MTT solution for 2 h at appropriate culture conditions. After incubation, the MTT solution was carefully removed, and formazan crystals were dissolved in DMSO (150 μL). Finally, the absorbance values were measured using a microplate reader at a wavelength of 570 nm [30].

Angiogenesis Co-culture Assay

The angiogenesis co-culture assay was used to investigate the roles and expressions of pro-angiogenesis factors (VEGF and FGF2). In our study, the co-culture assay developed by Bishop et al. was applied with slight modifications [31]. Specifically, 12-well transwell plates were used, in which the HUVECs at the density of 50,000/well were placed at the bottom, and the inserts were filled with a monolayer of HEC-1A cancer cells at a density of 10,000/insert. The cancer cells in the setup were treated with various samples, including free Keto, Keto-liposomes (termed as Keto-Lipo), bevacizumab (termed as mAb), as well as Keto, and bevacizumab co-loaded liposomes (termed as Combo-Lipo) for 24 h. All the treatment groups were maintained at the same dose of Keto at 0.5 μM and bevacizumab at 1 μg mL^{-1}. To further figure out the pro-angiogenesis effects of the exosome, extra exosomes at a density of 50,000/insert were used to investigate whether the additive exosome enhances the expression of pro-angiogenesis factors. After 24 h, the inserts were removed, and the cell medium of bottom HUVECs was collected and measured with an ELISA kit, respectively (Human VEGF Quantikine ELISA KitCatalog #: DVE00, Human FGF basic/FGF2/bFGF Quantikine ELISA Kit Catalog #: DFB50, R&D systems, Minneapolis, USA).

Co-culture Assay of Cancer Cells with Fibroblasts

The Trans-well system was co-cultured using fibroblasts with HEC-1A cancer cells. Briefly, a 12-well transwell plate was applied for the assay. In this setup, the bottom of each well was seeded with primary human fibroblast at a density of 50,000 cells per well. The insert of the transwell plate contained a monolayer of HEC-1A cancer cells at a density of 10,000 cells per insert. Further, the corresponding wells were treated with free Keto, Keto-Lipo, bevacizumab (mAb), and Combo-Lipo (liposomes co-loaded with Keto

Table 1 The optimization of the formulation for liposome preparation

Formulation	Encapsulation effiency (%)	Drug loading (%)
F1 DOPC:CHOL:DSPE-PEG:Keto = 6:2:1:0.5	91.3 ± 2.3	3.3 ± 0.08
F2 DOPC:CHOL:DSPE-PEG:Keto = 6:2:1:1	84.6 ± 3.1	6.04 ± 0.21
F3 DOPC:CHOL:DSPE-PEG:Keto = 6:2:1:1.5	51.6 ± 1.04	7.65 ± 0.15

and bevacizumab). All the treatment groups were maintained with the same dose of Keto at 0.5 μM and bevacizumab at 1 μg mL^{-1}. After 24 h, the inserts were removed, and the cells in the bottom chamber were collected. The mRNA of MMP3 and HGF expression levels were obtained using the quantitative reverse-transcriptase-polymerase chain reaction (qRT-PCR) analysis.

qRT-PCR Analysis

The qRT-PCR assay was performed using the following procedure. Briefly, the total RNA was extracted from the samples using a commercially available ribose nucleic acid (RNA) extraction kit (QIAwave RNA Mini Kit (250) Cat. No./ID: 74536), according to the manufacturer's instructions. The concentration and purity of the extracted RNA were determined using a nanodrop instrument. Further, the complimentary deoxyribose nucleic acid (cDNA) synthesis was carried out using a reverse transcription kit (100) Cat. No./ID: RT31-100 (Qiangen, Co. Ltd. Hilden, Germany). The reaction mixture included extracted RNA, reverse transcriptase buffer, dNTPs, RNase inhibitor, and reverse transcriptase enzyme. The thermal cycling conditions for cDNA synthesis were as follows: 25 °C for 5 min, 42 °C for 60 min, and 85 °C for 5 min. Finally, the RNA was isolated using the kit. Finally, the qRT-PCR amplification was performed on a real-time PCR system (7500 Fast) using the specific primers and SYBR Green master mix. The reaction mixture consisted of a cDNA template, forward and reverse primers, and SYBR Green master mix. MMP3 Human qPCR Primer Pair (NM_002422):

Forward—CACTCACAGACCTGACTCGGTT
Reverse—AAGCAGGATCACAGTTGGCTGG

HGF Human qPCR Primer Pair (NM_000601)—HP200568.

Forward—GAGAGTTGGGTTCTTACTGCACG
Reverse—CTCATCTCCTCTTCCGTGGACA

β-Actin (ACTB) Human qPCR Primer Pair (NM_001101).

Forward—CACCATTGGCAATGAGCGGTTC
Reverse—AGGTCTTTGCGGATGTCCACGT

The qRT-PCR cycling conditions were set as follows. Following the specified PCR program, the primer mix was tested to produce reliable qRT-PCR data using the ABI 7900HT instrument. Stage 1 involved an activation step at 50 °C for 2 min. Stage 2 included a pre-soaking at 95 °C for 10 min. Stage 3 comprised denaturation at 95 °C for 15 s, followed by annealing at 60 °C for 1 min. Stage 4 involved a melting curve analysis with cycles of 95 °C for 15 s, 60 °C for 15 s, and 95 °C for 15 s.

Effect of Liposomes on T-Cell Co-cultured with Cancer Cell

Cancer cells were co-cultured with human T-cells using the following procedure. Before the assay, all T-cells were activated by the addition of NanoSpark™ STEM-T Soluble T-Cell Activator. Then, similar procedures for the co-culture and cancer cells were received for the treatments, including free Keto, keto-liposomes, bevacizumab, Keto, and bevacizumab co-loaded liposomes for 24 h. The T-cells at a density of 200,000/well were settled in the bottom chamber of a 12-well plate. The cancer cells were seeded in a 12-well plate at a density of 10,000 cells per insert. Eventually, the T-cells were collected, and cell supernatant was obtained after the centrifugation. The production of cytokines IFN-γ was measured using the ELISA kit (Human IFN-gamma Quantikine ELISA Kit catalog: DIF50C, R&D system).

In Vivo Anti-tumor Efficacy and Biosafety of Liposomes

Female BALB/C mice aged 6 to 8 weeks were used for the in vivo investigations. The animal-related experiments were observed and approved by the Institutional Animal Ethical Committee of our hospital. Initially, an orthotopic xenograft model was established by injecting 1×10^6 HEC-1A cells onto the dorsal side of the mice. Once the tumor volume reached 100 mm^3, the mice were randomly distributed into four treatment groups, each containing six mice. The treatment groups included control (PBS), Keto-Lipo, the mAb, and Combo-Lipo, administered intravenously with an injection dose of 100 μL every 2 days. Notably, the concentration of Keto was 5 mg kg^{-1}, while the concentration of mAb was 0.5 mg kg^{-1}. The body weight and tumor volume were measured every 2 days.

Statistical Analysis

Data were presented as the mean ± standard deviation (S.D.). The differences between the data were compared using the one-way analysis of variance (ANOVA), followed by post-hoc Tukey's test, considering the P value lesser than 0.05 as statistically significant. * Signifies $P < 0.05$, ** indicates $P < 0.01$, and *** represents $P < 0.001$.

Results

Characterizations of Liposomes

Initially, the designed novel Combo-Lipo was thoroughly characterized to assess its potential as a therapeutic formulation. The particle size distribution of the Combo-Lipo

revealed a uniform distribution with an average size of approximately 100 nm (Fig. 1A). The optimal size range could be ideal for drug delivery applications, enabling efficient biodistribution in the bloodstream and cellular internalization. Further, the colloidal stability of Combo-Lipo formulation in serum was assessed to determine its ability to maintain particle integrity and prevent premature degradation in the biological environment. It was observed that the Combo-Lipo formulation exhibited excellent serum stability, as only minimal changes were evidenced in the average particle size after 72 h at 37 °C (Fig. 1B). Besides optimal particle size, this serum stability in the physiological fluids plays a crucial role in ensuring the sustained release and subsequent therapeutic efficacy of the encapsulated drug upon administration. In addition, the long-term physical stability of Combo-Lipo in serum-free condition at 4 °C was investigated to evaluate its shelf-life and storage potential. Similar to physiological stability, the formulation exhibited remarkable physical stability after 20 days at 4 °C, with no significant changes in the average particle size (Fig. 1C).These results indicated that the Combo-Lipo formulation could be stored for extended periods without compromising its structural integrity or therapeutic potential. Apart from the particle size, the amount of drug remaining in the formulation after the incubation period in the long-term stability assays plays a crucial role in assessing the encapsulation ability and subsequent performance of the Combo-Lipo formulation. The results revealed no significant change in the drug concentration, indicating that the Combo-Lipo effectively preserved the drug payload over time, maintaining its therapeutic activity (Fig. 1D). The drug release profile showed a sustained drug release (Fig. 1E).

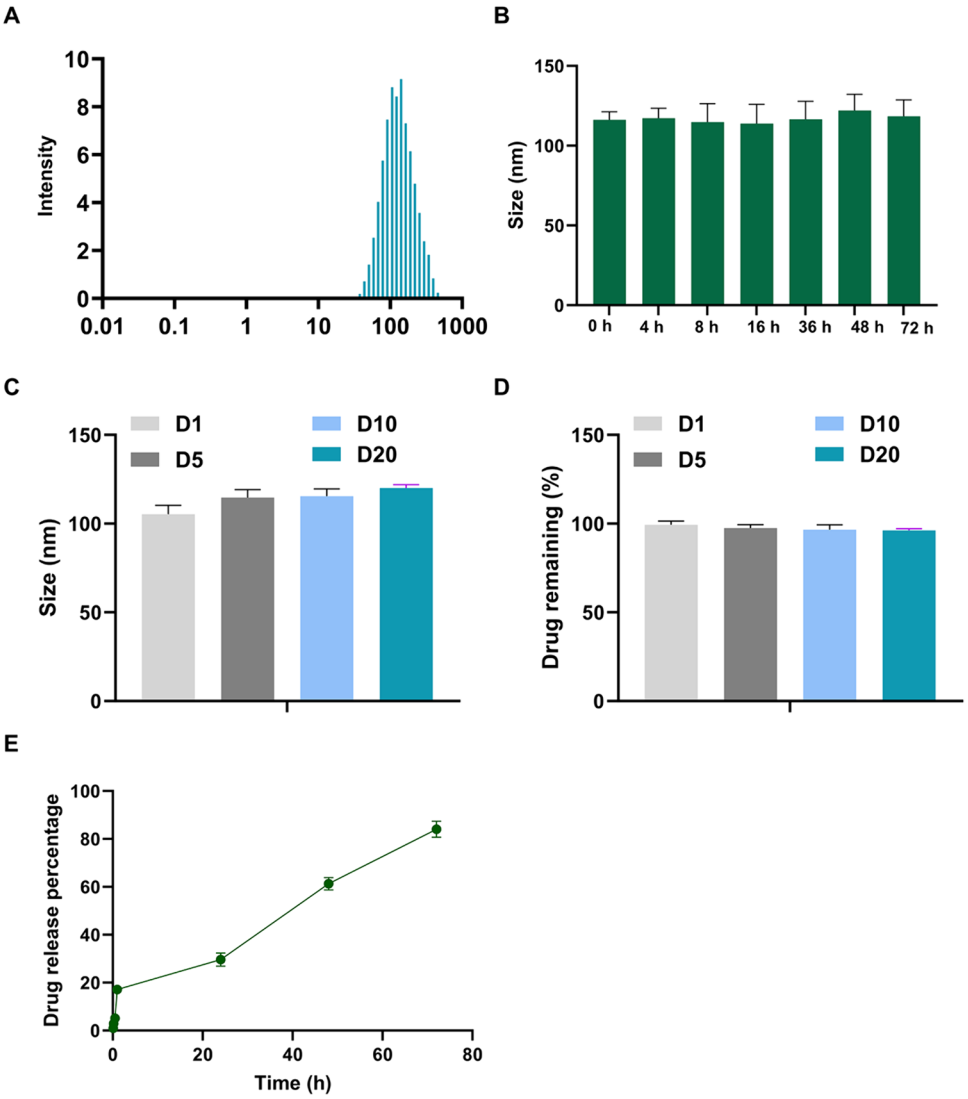

Fig. 1 Characterizations of the Combo-Lipo formulation. **A** The particle size distribution of Combo-Lipo. **B** Serum stability of Combo-Lipo indicated by the particle size. **C** Long-term physical stability of Combo-Lipo. **D** Drug remaining percentage in the long-term stability assays. **E** Drug release profile. Data are presented as the mean ± S.D. ($n = 3$)

Anti-cancer Efficacy In Vitro

Further, the effect of different Combo-Lipo treatments on the viabilities of cells was evaluated using three different endometrial cancer cell lines, i.e., HEC-1B, HEC-1A, and RL95-2. In these endometrial cancer cell lines, the viabilities of cells were assessed after 48 h of treatment with various interventions, such as I—control, II—vehicle, III—free Keto, IV—bevacizumab, V—Keto-Lipo + bevacizumab, and VI—Combo-Lipo. It was observed that all the cell lines showed the order of viability of cells, as control > vehicle > free Keto > bevacizumab > Keto-Lipo + bevacizumab > Combo-Lipo, indicating the most potent effect of final Combo-Lipo formulation in reducing cell viability of all endometrial cell lines (Fig. 2A–C). The results demonstrated that the designed liposomal formulations, i.e., Combo-Lipo and Keto-Lipo + bevacizumab, led to significantly lower viabilities of cells in all the endometrial cell lines compared to the free drug treatments, i.e., Keto and bevacizumab. More importantly, free bevacizumab showed increased potency over the free Keto, indicating the efficacy of the monoclonal antibody. Considering the bevacizumab efficacy, Lipo-Keto combined with bevacizumab was treated in all the cell lines, indicating excellent therapeutic efficacy. The higher efficacy of Lipo-Keto combined with bevacizumab than free drugs could be due to increased biodistribution and solubility of Keto from liposomal formulation efficacy. These results indicated that liposomes exerted a more significant impact on reducing the viabilities of all cells. Further, the colony-forming assay indicated that Keto-Lipo inhibited cell proliferation. In addition, the bevacizumab treatment showed similar inhibitory effects. Cumulatively, the synergetic liposome formulations showed the most potent effects (Fig. 2D). Together, these liposomal formulations presented exceptional therapeutic effects, possibly due to improved liposome internalization into cell lines.

Downregulation of Angiogenic Factors

Several angiogenic factors play important roles in cancer development through participating in neovascularization. In this vein, several angiogenic mediators include vascular endothelial growth factor (VEGF) and fibroblast growth factor 2 (FGF2). Inhibiting the expression of such angiogenic mediators would substantially benefit the prevention of metastasis [23]. Moreover, CAF-mediated ECM remodeling is critical in facilitating tumor invasion and metastasis. In addition, the transforming growth factor-β (TGF-β), hepatocyte growth factor (HGF), specific interleukins, and metalloproteases are some of the secreted key components involved in this ECM remodeling process. These factors can be targeted for cancer therapy, termed as CAF-targeted therapy. This CAF-targeted therapy holds promising potential as one of the innovative therapeutic approaches. The inhibitory effects of liposomes on pro-angiogenic factors genes were investigated in the co-culture system of cancer cells and fibroblasts. Accordingly, MMP-3, an important metalloprotease involved in ECM remodeling, was analyzed after

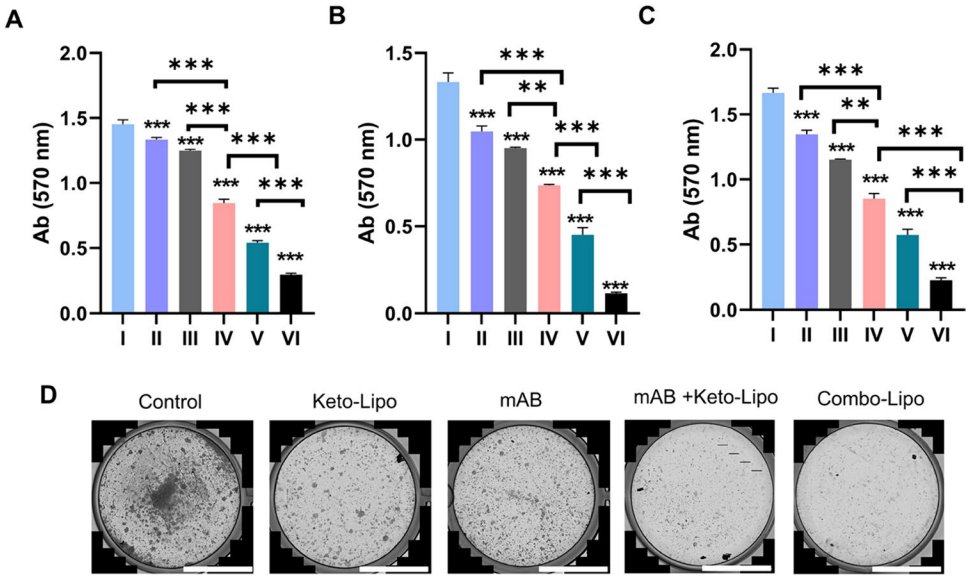

Fig. 2 The impact of different treatments on various cancer cell viability. **A** The cell viability of HEC-1B cancer cell line with different treatments for 48 h. **B** The cell viability of HEC-1A cancer cell line with different treatments for 48 h. **C** The cell viability of RL95-2 cancer cell line with different treatments for 48 h. (I—control group, II—vehicle, III—free Keto, IV—bevacizumab, V—Keto-Lipo + bevacizumab, and VI—Combo-Lipo. Data are presented as the mean ± S.D. ($n = 3$) analyzed by one-way analysis of variance (ANOVA). ** Indicates $P < 0.01$, and *** represents $P < 0.001$) **D** The cell colony of HEC-1A under different treatment interventions (Scale bar: 1000 µm)

24 h of treatment with different formulations. The results revealed a significant decrease in the MMP-3 expression following treatment with liposomes, suggesting their potential to inhibit the ECM remodeling and reduce tumor invasiveness in the co-culture system (Fig. 3A).

Moreover, the expression of HGF-1α, a key factor secreted by fibroblasts, was evaluated in the co-culture system treated with different formulations. HGF expression was assessed in different experimental groups consisting of normal fibroblasts, cancer cells in the insert, cancer cells + free Keto, cancer cells + Keto-Lipo, cancer cells + bevacizumab, and cancer cells + Combo-Lipo. The experimental data revealed a significant reduction in the HGF mRNA expression in the experimental groups treated with liposomes compared to the other groups. These findings suggested that liposome-based formulations might effectively target HGF and potentially impede the pro-metastatic effects of fibroblast-secreted factors in the co-culture system (Fig. 3B).

Further, the migration and invasion abilities of HECA-1 were observed after treatment with different formulations. It was observed that the free Keto failed to achieve similar inhibitory effects as the Keto-Lipo, which could be attributed to the poor solubility of free Keto. Moreover, we noticed that, even with the usage of DMSO for improving solubility, the Keto treatment group still resulted in minor precipitation, affecting the distribution in the wells. Noticeably, the Keto-based liposomal formulation drastically improved the anti-migration effects of Keto, indicating the inhibition of exosome release benefitting the anti-migration efficacy. Like cell proliferation, the VEGF antibody, i.e., bevacizumab, exhibited favorable inhibition of migration and invasion abilities of the cell line. As anticipated, the combo-Lipo group showed the most potent effect among all the treatment groups (Fig. 3C, D).

In the TME, the hypoxia factors (such as hypoxia-inducible factor, HIF-1α) disrupt the balance of angiogenic factors, favoring the release of pro-angiogenic factors [24]. The release of various pro-angiogenic factors (VEGF and FGF-2) happens to be through local signaling (paracrine) and self-stimulation (autocrine) mechanisms [25]. The co-culture assays indicated that cancer cells significantly elevated the levels of these important inducers of angiogenesis, namely VEGF and FGF2. Notably, these growth factors play crucial roles in promoting the formation of new blood vessels. However, the levels of VEGF and FGF2 were effectively reduced after treatment with a particular intervention. Among different treatment groups, the combination therapy (Combo-Lipo) demonstrated the most potential therapeutic effects in downregulating the expression levels of VEGF and FGF2, indicating a synergistic effect in suppressing the production of these angiogenic factors by the cancer cells. Interestingly, it was observed that the presence of additional exosomes led to an increased production of FGF2. Exosomes are small extracellular vesicles involved in intercellular communication between cells, enhancing the production of FGF2 by the cancer cells. Furthermore, the Keto-Lipo treatment involving liposomes containing Keto substantially reduced the upregulated expression levels of VEGF and FGF2 proteins. These results suggested that Keto-Lipo presented an exceptional anti-angiogenic effect, effectively countering the pro-angiogenic impact of exosomes.

Inhibition of TAMs

TAMs belong to a specific family of immune cells that infiltrate the TME, which play crucial roles in tumor progression and immune suppression [26]. Among various TAM subtypes, M2 macrophages are crucial in releasing tumor-promoting factors, such as TGF-β and interleukin-10 (IL-10) (Fig. 4A, B). These factors often contribute to creating an immunosuppressive TME, promoting epithelial-mesenchymal transition (EMT), stimulating angiogenesis, and facilitating ECM remodeling [27]. The immunosuppressive TME created by M2 macrophages is partly mediated by the release of TGF-β and IL-10 expression, hindering effective anti-tumor immune responses. Moreover, these factors promote the transformation of cancer cells into a more invasive and metastatic phenotype through EMT. Besides, the stimulation of angiogenesis by M2 macrophage-released factors supports the growth and survival of the tumor by facilitating the formation of new blood vessels. Moreover, M2 macrophages contribute to the remodeling of the ECM, promoting tumor invasion and metastasis. Considering these aspects, we then studied the activity of M2 TAM. It was observed from the results that the M2 TAM activity was inhibited by the decrease of these tumor-promoting factors via blocking exosome-mediated communication. These findings suggested that the potential of Keto-Lipo could be the reason for enhancing cancer treatment outcomes. In addition, the Combo-Lipo treatment showed the most potent inhibitory role in exploring their anti-cancer effect.

Effect of Liposomes on Angiogenesis Factors

Furthermore, the ELISA analysis revealed the concentrations of these FGF2 and VEGF proteins in the samples, providing insights into their expression or secretion. The ELISA analysis showed an FGF2 concentration of X ng mL^{-1}. The resultant amount of FGF2 protein might certainly play a role in various cellular processes, such as cell growth, proliferation, and angiogenesis. To this end, the resultant VEGF levels by the ELISA analysis indicated Y ng mL^{-1} in the samples. The measured concentration of VEGF would be appropriate for its potential involvement in angiogenic processes and its impact on tumor growth, wound healing, and other physiological or pathological conditions. These quantitative results

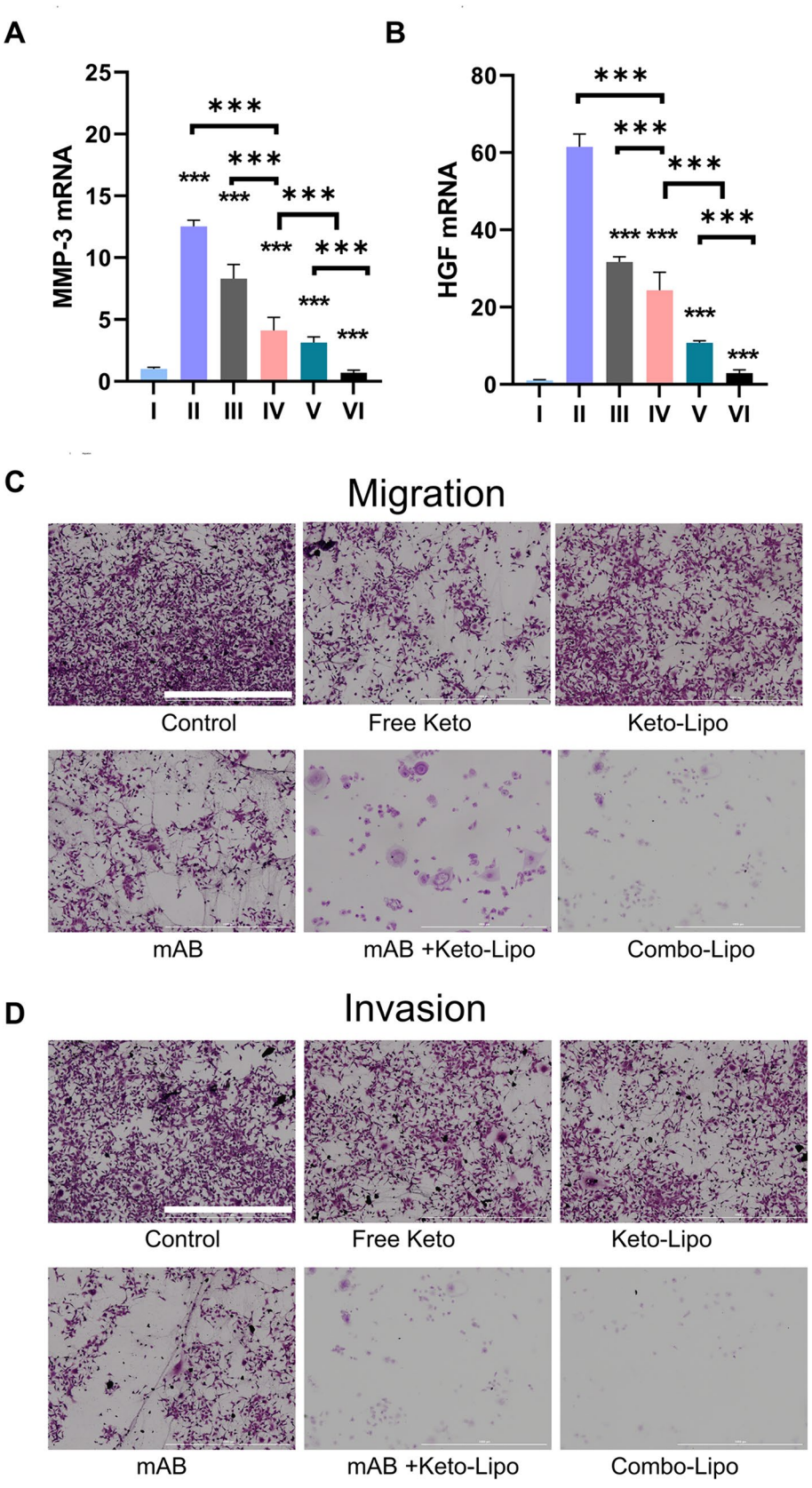

Fig. 3 Effect of liposomal formulations on pro-angiogenic factors genes. **A** The changes in the expression levels of MMP-3 in co-culture systems treated with different formulations for 24 h. (Cancer cells in the insert and normal fibroblast in the bottom). **B** HGF expression levels in the co-culture systems treated with different formulations for 24 h. (I—normal fibroblasts, II—cancer cells in the insert, III—cancer cells + free Keto, IV—cancer cells + Keto-Lipo, V—cancer cells + bevacizumab, and VI—cancer cells + Combo-Lipo). Data are presented as the mean ± S.D. ($n = 3$). ** Indicates $P < 0.01$, and *** represents $P < 0.001$, one-way ANOVA. **C** Migration ability of HEC-1A cells under different treatments. **D** Cell invasion assay of HEC-1A under different treatment exposures (Scale bar: 1000 µm)

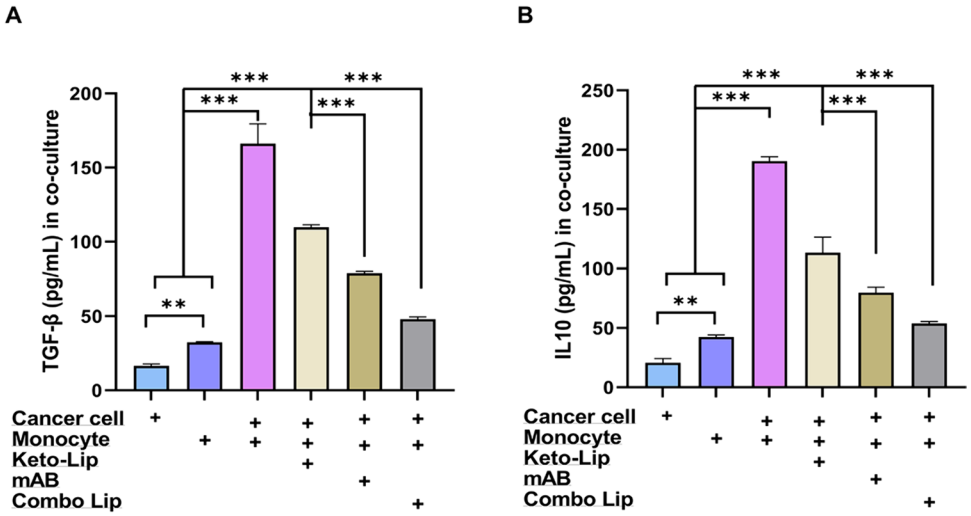

Fig. 4 Effect of liposomes on TAM biomarkers. The cytokines, i.e., **A** TGF-β (M2 marker) and **B** IL-10 (M2 marker) in cancer cells and monocyte co-culture system. The data ($n = 3$) were analyzed using one-way ANOVA. ** Indicates $P < 0.01$ and *** presents $P < 0.001$

obtained from the ELISA analysis offer valuable insights in contributing to our understanding of the roles of these proteins in specific biological processes, disease mechanisms, or the evaluation of therapeutic interventions targeting FGF2 and VEGF (Fig. 5A, B). In addition, the CD31 expression was determined by the immunofluorescence staining after treatment with various liposomal formulations and pure drugs. As depicted in Fig. 5C, the expression level of tumor microvessel biomarker CD31 was reduced in the therapeutic liposome group.

Anti-cancer Investigations In Vivo

Before performing in vivo investigations, we explored the efficacy of using the 3D tumor spheres in vitro to minimize the usage of mice. It was observed from the experimental results that the blank liposome treatment showed minor sphere growth efficacy. On the other hand, due to the limited penetration of free Keto, the free Keto treatment exhibited minor inhibitory effects in the 3D model, similar to the control group (Fig. 6A). Among various treatment groups, the combinational group, i.e., Combo-Lipo, presented the most potent inhibitory effects. Thus, in vivo investigations were designed and executed using the four groups, including phosphate-buffered saline (PBS) as the control group, as well as the Keto-Lipo, mAb, and Combo-Lipo as experimental groups. To assess their efficacy and tolerability, the anti-cancer effects of the designed formulations were evaluated using a xenograft model in nude mice. After treatment, the two key parameters of tumor and body weights were measured to gauge the impact of different treatments.

Regarding the tumor weights, the tumors were excised from the mice after different treatment interventions and compared the weights of the tumors. The results unequivocally demonstrated a significant reduction in the tumor weights in the Combo-Lipo treatment group compared to the other treatment groups. The treatment outcome indicated that Combo-Lipo inhibited tumor growth in the xenograft model. In addition to tumor weights, the body weight of the mice was closely monitored during the treatment duration to evaluate any potential adverse effects or toxicity associated with the administered treatments. Encouragingly, the experimental results revealed that the mice treated with Combo-Lipo showed insignificant changes in body weight compared to the control group. These findings suggested that Combo-Lipo was well-tolerated by the mice, inducing no notable weight loss or other detrimental effects and underscoring its favorable safety profile. These in vivo findings provided compelling evidence for the anti-cancer efficacy of Combo-Lipo in the xenograft model, as evidenced by the significant reduction in the tumor weights. Moreover, the well-tolerated nature of the Combo-Lipo formulation, as indicated by the stable body weight of the treated mice, further supported its promising potential to combat cancer (Fig. 6B, C).

IFN-γ, one of the potential cytokines, plays a vital role in anti-tumor immune responses by promoting immune cell activation, enhancing antigen presentation, and exerting direct anti-cancer effects [28]. Further, we analyzed the concentration of IFN-γ using the corresponding ELISA kit in the co-culture of T-cells and endometrial cancer cells, revealing a level of approximately 41 pg mL^{-1} in the co-culture cell

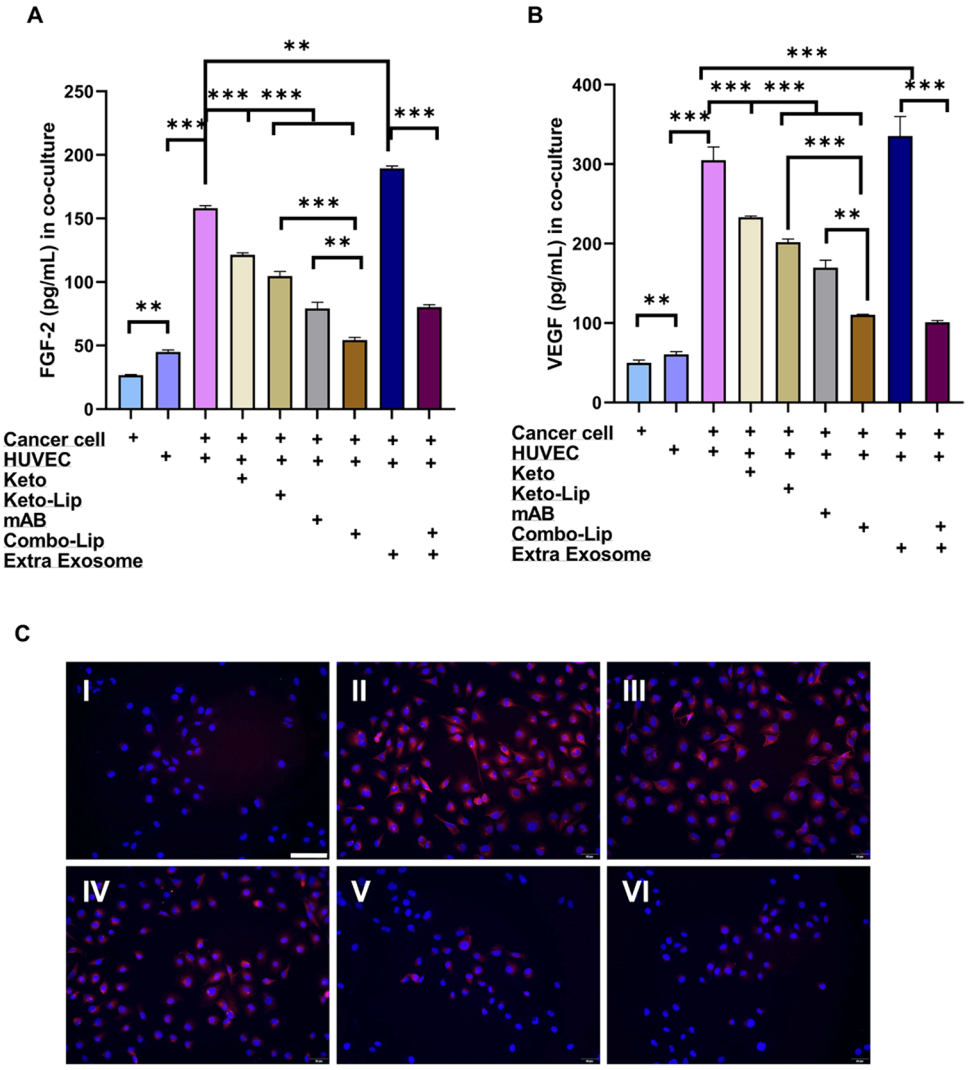

Fig. 5 The inhibitory effects of liposomes on angiogenesis. The expression levels of **A** FGF-2 and **B** VEGF in cancer cells and human umbilical vein endothelial cells (HUVECs) co-culture system by ELISA analysis ($n=3$). ** Indicates $P<0.01$ and *** presents $P<0.001$. **C** The inhibitory effects of liposome treatment on CD31 expression levels. (I—HUVECs control, II—HUVECs + cancer cells, III—HUVECs + cancer cells + blank liposomes, IV—HUVECs + extra exosomes, V—HUVECs + cancer cells + Keto-Lipo, and IV—HUVECs + cancer cell + Combo-Lipo). (Scale bar: 100 μm)

system. These findings suggested that cancer cells in the TME could decrease IFN-γ levels, potentially impairing the anti-tumor immune responses. Further, various liposomal formulations were employed to investigate the modulation of the levels of IFN-γ in the co-culture system. Among these treatments, the most pronounced effects were observed in the Combo-Lipo treatment group, followed by the Keto-Lipo or mAb treatment groups. These findings highlighted the potential of liposomes to enhance the production of IFN-γ in the co-culture system of T-cells and cancer cells. The increased levels of IFN-γ provided important insights into the impact of the interactions between these cell types, suggesting potential restoration or augmentation of anti-tumor immune responses. The experimental results could enable an understanding of the mechanisms underlying immune evasion by cancer cells and for exploring therapeutic interventions aimed at enhancing IFN-γ production (Fig. 6D).

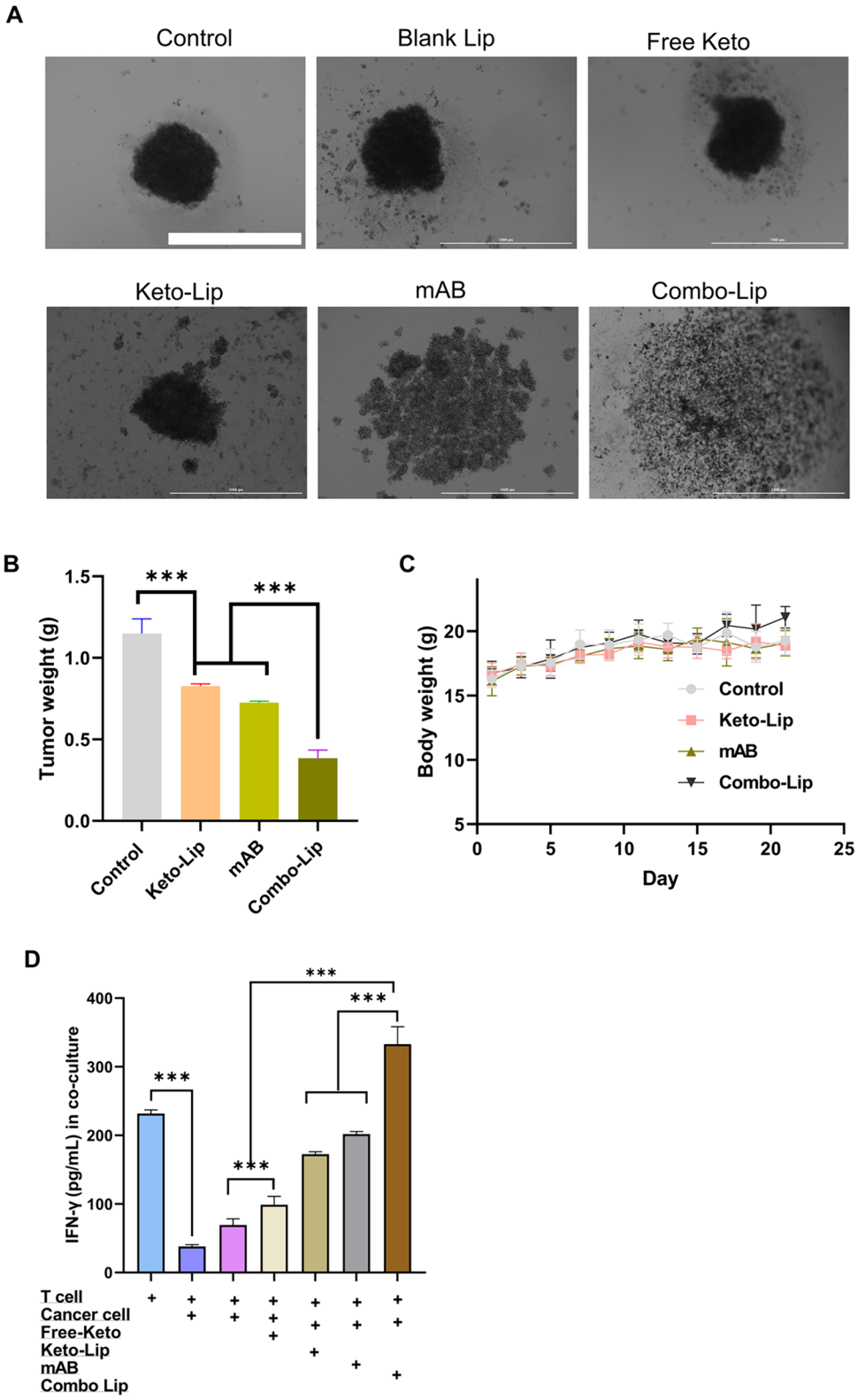

Fig. 6 Anti-cancer effects of Combo-Lipo in xenograft model. **A** 3D tumor sphere photos after various treatments. (Scale bar: 300 μm). **B** Tumor weights of xenograft mice after different treatments in the end-point. **C** The body weights of mice during the treatment time. *** Presents $P < 0.001$. **D** The cytokines of IFN-γ in cancer cells and T-cell co-culture system in the presence or absence of liposomes. *** Presents $P < 0.001$

Acknowledgements Not applicable.

Funding Not applicable.

Data Availability All data can be obtained by email request from the corresponding author.

Declarations

Competing Interests All authors have declared no competing interests.

Ethical Approval This study was approved by the Yantai Yuhuangding Hospital.

References

1. Morice, P., Leary, A., Creutzberg, C., Abu-Rustum, N., & Darai, E. (2016). Endometrial cancer. *The Lancet, 387*(10023), 1094–1108.
2. Jabbari, N., Akbariazar, E., Feqhhi, M., Rahbarghazi, R., & Rezaie, J. (2020). Breast cancer-derived exosomes: Tumor progression and therapeutic agents. *Journal of Cellular Physiology, 235*(10), 6345–6356.
3. Tetta, C., Ghigo, E., Silengo, L., Deregibus, M. C., & Camussi, G. (2013). Extracellular vesicles as an emerging mechanism of cell-to-cell communication. *Endocrine, 44*, 11–19.
4. Thakur, A., Parra, D. C., Motallebnejad, P., Brocchi, M., & Chen, H. J. (2022). Exosomes: Small vesicles with big roles in cancer, vaccine development, and therapeutics. *Bioactive Materials, 10*, 281–294.
5. Wu, Q., Zhou, L., Lv, D., Zhu, X., & Tang, H. (2019). Exosome-mediated communication in the tumor microenvironment contributes to hepatocellular carcinoma development and progression. *Journal of Hematology & Oncology, 12*(1), 1–11.
6. Maacha, S., Bhat, A. A., Jimenez, L., Raza, A., Haris, M., Uddin, S., & Grivel, J.-C. (2019). Extracellular vesicles-mediated intercellular communication: Roles in the tumor microenvironment and anti-cancer drug resistance. *Molecular Cancer, 18*, 1–16.
7. Peinado, H., Lavotshkin, S., & Lyden, D. (2011). The secreted factors responsible for pre-metastatic niche formation: Old sayings and new thoughts. *Seminars in Cancer Biology, 21*, 139–146.
8. Xu, T., Yu, S., Zhang, J., & Wu, S. (2021). Dysregulated tumor-associated macrophages in carcinogenesis, progression and targeted therapy of gynecological and breast cancers. *Journal of Hematology & Oncology, 14*(1), 1–20.
9. Franco, O. E., Shaw, A. K., Strand, D. W., & Hayward, S. W. (2010). Cancer associated fibroblasts in cancer pathogenesis. *Seminars in Cell & Developmental Biology, 21*, 33–39.
10. Kalluri, R., & Zeisberg, M. (2006). Fibroblasts in cancer. *Nature Reviews Cancer, 6*(5), 392–401.
11. Rundhaug, J. E. (2005). Matrix metalloproteinases and angiogenesis. *Journal of Cellular and Molecular Medicine, 9*(2), 267–285.
12. Chen, K., Xu, M., Lu, F., & He, Y. (2023). Development of matrix metalloproteinases-mediated extracellular matrix remodeling in regenerative medicine: A mini review. *Tissue Engineering and Regenerative Medicine, 20*, 1–10.
13. Yang, X., Li, Y., Zou, L., & Zhu, Z. (2019). Role of exosomes in crosstalk between cancer-associated fibroblasts and cancer cells. *Frontiers in Oncology, 9*, 356.
14. Lim, D., Do, Y., Kwon, B. S., Chang, W., Lee, M.-S., Kim, J., & Cho, J. G. (2020). Angiogenesis and vasculogenic mimicry as therapeutic targets in ovarian cancer. *BMB Reports, 53*(6), 291.
15. Ahmadi, M., & Rezaie, J. (2020). Tumor cells derived-exosomes as angiogenenic agents: Possible therapeutic implications. *Journal of Translational Medicine, 18*(1), 1–17.
16. Geindreau, M., Bruchard, M., & Vegran, F. (2022). Role of cytokines and chemokines in angiogenesis in a tumor context. *Cancers, 14*(10), 2446.
17. Cao, J., Liu, X., Yang, Y., Wei, B., Li, Q., Mao, G., He, Y., Li, Y., Zheng, L., & Zhang, Q. (2020). Decylubiquinone suppresses breast cancer growth and metastasis by inhibiting angiogenesis via the ROS/p53/BAI1 signaling pathway. *Angiogenesis, 23*, 325–338.
18. Parvathaneni, V., Kulkarni, N. S., Muth, A., & Gupta, V. (2019). Drug repurposing: A promising tool to accelerate the drug discovery process. *Drug Discovery Today, 24*(10), 2076–2085.
19. Yang, Z., Deng, W., Zhang, X., An, Y., Liu, Y., Yao, H., & Zhang, Z. (2022). Opportunities and challenges of nanoparticles in digestive tumours as anti-angiogenic therapies. *Frontiers in Oncology, 11*, 5581.
20. Zhigaltsev, I. V., & Cullis, P. R. (2023). Morphological behavior of liposomes and lipid nanoparticles. *Langmuir, 39*(9), 3185–3193.
21. Noh, G., Keum, T., Bashyal, S., Seo, J.-E., Shrawani, L., Kim, J. H., & Lee, S. (2022). Recent progress in hydrophobic ion-pairing and lipid-based drug delivery systems for enhanced oral delivery of biopharmaceuticals. *Journal of Pharmaceutical Investigation, 52*, 1–19.
22. Wang, S., Chen, Y., Guo, J., & Huang, Q. (2023). Liposomes for tumor targeted therapy: A review. *International Journal of Molecular Sciences, 24*(3), 2643.
23. Calviello, G., Di Nicuolo, F., Gragnoli, S., Piccioni, E., Serini, S., Maggiano, N., Tringali, G., Navarra, P., Ranelletti, F. O., & Palozza, P. (2004). n-3 PUFAs reduce VEGF expression in human colon cancer cells modulating the COX-2/PGE 2 induced ERK-1 and-2 and HIF-1α induction pathway. *Carcinogenesis, 25*(12), 2303–2310.
24. Tang, Y.-A., Chen, Y.-F., Bao, Y., Mahara, S., Yatim, S. M. J., Oguz, G., Lee, P. L., Feng, M., Cai, Y., & Tan, E. Y. (2018). Hypoxic tumor microenvironment activates GLI2 via HIF-1α and TGF-β2 to promote chemoresistance in colorectal cancer. *Proceedings of the National Academy of Sciences, 115*(26), E5990–E5999.
25. Ghalehbandi, S., Yuzugulen, J., Pranjol, M. Z. I., & Pourgholami, M. H. (2023). The role of VEGF in cancer-induced angiogenesis and research progress of drugs targeting VEGF. *European Journal of Pharmacology, 949*, 175586.
26. Mao, X., Xu, J., Wang, W., Liang, C., Hua, J., Liu, J., Zhang, B., Meng, Q., Yu, X., & Shi, S. (2021). Crosstalk between cancer-associated fibroblasts and immune cells in the tumor microenvironment: New findings and future perspectives. *Molecular Cancer, 20*(1), 1–30.

27. Chen, Y., Tan, W., & Wang, C. (2018). Tumor-associated macrophage-derived cytokines enhance cancer stem-like characteristics through epithelial–mesenchymal transition. *OncoTargets and Therapy, 11*, 3817–3826.
28. Li, W.-S., Chu, C.-L., Chen, M.-H., Lu, Y.-S., Lai, J.-S., You, B.-J., & Lin, C.-C. (2018). *Lepista sordida* water extract enhances the maturation of mouse dendritic cells in vitro and in vivo. *Iranian Journal of Immunology, 15*(4), 256–268.
29. Kang, X.-J., Wang, H.-Y., Peng, H.-G., Chen, B.-F., Zhang, W.-Y., Wu, A.-H., Xu, Q., & Huang, Y.-Z. (2017). Co-delivery of dihydroartemisinin and doxorubicin in mannosylated liposomes for drug-resistant colon cancer therapy. *Acta Pharmacologica Sinica, 38*(6), 885–896.
30. Mo, X., Zheng, Z., He, Y., Zhong, H., Kang, X., Shi, M., Liu, T., Jiao, Z., & Huang, Y. (2018). Antiglioma via regulating oxidative stress and remodeling tumor-associated macrophage using lactoferrin-mediated biomimetic co-delivery of simvastatin/fenretinide. *Journal of Controlled Release, 287*, 12–23.
31. Bishop, E. T., Bell, G. T., Bloor, S., Broom, I., Hendry, N. F., & Wheatley, D. N. (1999). An in vitro model of angiogenesis: Basic features. *Angiogenesis, 3*, 335–344.